

RESEARCH ARTICLE

Alternative vaccine administration by powder injection: Needle-free dermal delivery of the glycoconjugate meningococcal group Y vaccine

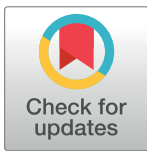
Nikolas T. Weissmueller^{1,2,3}*, Leanne Marsay¹, Heiko A. Schiffter³, Robert C. Carlisle³, Christine S. Rollier¹, Robert K. Prud'homme², Andrew J. Pollard¹

1 Department of Paediatrics, Oxford Vaccine Group, University of Oxford and the NIHR Oxford Biomedical Research Institute, Oxford, Oxfordshire, United Kingdom, **2** Department of Biological and Chemical Engineering, Princeton University, Princeton, New Jersey, United States of America, **3** Institute of Biomedical Engineering, Biomedical Ultrasonics, Biotherapy & Biopharmaceuticals Laboratory (BUBBL), Oxford, Oxfordshire, United Kingdom

* These authors contributed equally to this work.

✉ Current address: Department of Applied Natural Science, University of Applied Sciences, Cologne, North Rhine-Westfalia, Germany.

* ntw@princeton.edu



OPEN ACCESS

Citation: Weissmueller NT, Marsay L, Schiffter HA, Carlisle RC, Rollier CS, Prud'homme RK, et al. (2017) Alternative vaccine administration by powder injection: Needle-free dermal delivery of the glycoconjugate meningococcal group Y vaccine. PLoS ONE 12(8): e0183427. <https://doi.org/10.1371/journal.pone.0183427>

Editor: Eliane N. Miyaji, Instituto Butantan, BRAZIL

Received: May 19, 2017

Accepted: August 3, 2017

Published: August 24, 2017

Copyright: © 2017 Weissmueller et al. This is an open access article distributed under the terms of the [Creative Commons Attribution License](https://creativecommons.org/licenses/by/4.0/), which permits unrestricted use, distribution, and reproduction in any medium, provided the original author and source are credited.

Data Availability Statement: The authors confirm that all data underlying the findings are fully available without restriction. All relevant data are within the paper.

Funding: This work was supported by the Oxford Martin School, University of Oxford. URL: <http://www.oxfordmartin.ox.ac.uk/>. The funders had no role in study design, data collection and analysis, decision to publish, or preparation of the manuscript.

Abstract

Powder-injectors use gas propulsion to deposit lyophilised drug or vaccine particles in the epidermal and sub epidermal layers of the skin. We prepared dry-powder ($T_g = 45.2 \pm 0.5^\circ\text{C}$) microparticles ($58.1 \mu\text{m}$) of a MenY-CRM₁₉₇ glycoconjugate vaccine (0.5% wt.) for intradermal needle-free powder injection (NFPI). SFD used ultrasound atomisation of the liquid vaccine-containing excipient feed, followed by lyophilisation above the glass transition temperature ($T_g' = -29.9 \pm 0.3^\circ\text{C}$). This resulted in robust particles (density $\sim 0.53 \pm 0.09 \text{ g/cm}^3$) with a narrow volume size distribution (mean diameter $58.1 \mu\text{m}$, and span = 1.2), and an impact parameter (pvr $\sim 11.5 \text{ kg/m}\cdot\text{s}$) sufficient to breach the *Stratum corneum* (sc). The trehalose, mannitol, dextran (10 kDa), dextran (150 kDa) formulation, or TMDD (3:3:3:1), protected the MenY-CRM₁₉₇ glycoconjugate during SFD with minimal loss, no detectable chemical degradation or physical aggregation. In a capsular group Y *Neisseria meningitidis* serum bactericidal assay (SBA) with human serum complement, the needle free vaccine, which contained no alum adjuvant, induced functional protective antibody responses *in vivo* of similar magnitude to the conventional vaccine injected by hypodermic needle and syringe and containing alum adjuvant. These results demonstrate that needle-free vaccination is both technically and immunologically valid, and could be considered for vaccines in development.

Competing interests: AJP has previously conducted clinical trials of vaccines on behalf of Oxford University funded by vaccine manufacturers but did not receive any personal payments from them. His department received unrestricted educational grants from Pfizer/GSK/Astra Zeneca in July 2016 for a course on Infection and Immunity in Children. AJP is chair of the UK Department of Health's (DH) Joint Committee on Vaccination and Immunisation (JCVI), and a member of WHO's Strategic Advisory Group of Experts, but the views expressed in this manuscript do not necessarily represent the views of JCVI or DH or WHO. This does not alter our adherence to PLOS ONE policies on sharing data and materials. The other authors have declared that no competing interests exist.

Introduction

Most of the 800 million vaccine injections performed each year are administered by intramuscular needle and syringe injection [1]. There are a number of disadvantages associated with conventional needle administration, including the risk of transmission of blood-borne viruses (such as HIV), the need for large-scale disposal of needles [2–4]. Glycoconjugate vaccines comprise one or more polysaccharides of bacterial origin that are covalently linked to an immunogenic carrier protein [5]. They are thymus dependent vaccines, due to the protein carrier which recruits T cells to enhance the B cell response in germinal centres, and have substantially reduced the disease burden associated with polysaccharide-encapsulated bacteria, such as *Haemophilus influenzae* type b, *Streptococcus pneumoniae* and *Neisseria meningitidis* [6–8]. Meningococcal meningitis and septicaemia, caused by *Neisseria meningitidis* (Men) infection, involves invasion of the blood and meninges of the brain and spinal cord and is accompanied by devastating morbidity and mortality. The largest disease burden historically fell on sub-Saharan Africa, also known as the meningitis belt, where a large-scale program is underway to protect the population from further outbreaks [9]. Of the pre-existing vaccines, none have a needle-free alternative.

A plethora of vaccine delivery approaches achieve permeation or penetration of the *Stratum corneum* (*sc*) barrier. These include chemical permeability enhancers, ultrasound, electroporation, micro-needles, liquid-jet injection, and *sc* removal by tape-stripping among others [10–13]. The advantages and disadvantages of these methods have been previously summarized. While no single needle-free technology is likely to emerge as the most suitable choice for all clinical settings, the respective advantages and limitations of each technology will differentiate their suitability [12]. One advantage of powder injection is the use of well-established and readily scalable pharmaceutical formulation processes such as lyophilisation [14, 15].

Needle-free powder injection (NFPI) is a delivery modality that deposits vaccine or drug particles into the epidermal and sub epidermal layers of the skin [16, 17]. Ballistic injectors expose individual powder particles to high acceleration and deceleration forces, as experienced upon device actuation and particle impact on the skin [18]. Powder injector devices accelerate vaccine particles in the stream of expanding helium gas (at 30–60 bar pressure), and achieve velocities of up to 1050 m/s [19]. According to Kendall et al, the impact parameter (*prv*) required for particles to breach the *sc* ranges from 7–12 (kg/m·s) and is a function of particle density (ρ), radius (*r*) and velocity (*v*). [18] Generally, particles less than 100 μm in diameter have been reported as pain-free, while particles smaller than 20 μm were unable to penetrate into the epidermis [20]. If the overall amount of powder per injection is kept below 1–2 mg, bleeding can be almost entirely avoided [16].

The epidermis is difficult to target, but has several favourable immunogenic properties. Phenotypically immature Langerhans cells (LCs) line the epidermis in a network of cytoplasmic processes, which cover about 25% of the epidermal area. Upon contact with an antigen, LCs endocytose the antigen. Subsequently, LCs detach from their cytoplasmic network, and prompted by inflammatory cytokine cues of the surrounding keratinocytes, LCs migrate into the lymphatic system where they mature to antigen-presenting cells (APCs), before interacting with naïve T cells in the lymph nodes [21]. Interconnected components of the cutaneous immune response extend from the site of pathogen entry, to tissue homing antigen specific cell mediated immunity, to systemic immunity of the entire organism and confer an unique immunological potency to the skin, which renders it an especially appealing target for alternate immunization procedures such as needle-free powder injection that may potentiate and modulate the immune response [22, 23]

Since 2003, most investigational dry-powder formulations of viral and bacterial protein antigens for application in needle-free ballistic injection were manufactured by spray-freeze drying (SFD) [24]. Briefly, SFD atomizes a liquid formulation that conventionally contains an active pharmaceutical ingredient and various excipients into a cryogenic liquid prior to the removal of water from the frozen droplets by ice sublimation at reduced temperatures and pressures [25]. Relative to alternative particle manufacture methods, such as spray-drying or compaction and grinding, SFD readily produces particles with a larger diameter and a more narrow size distribution respectively [26, 27]. However, many small ice crystals form within single particles due to fast freezing rates, which upon sublimation results in a highly porous construct that mechanically is not suitable for ballistic injection [28–30]. The addition of a high solute content in the liquid feed, the addition of polymers such as dextran, or a temperature adjustment to the lyophilisation procedure may be used to reduce particle porosity and increase structural robustness of SFD powders [15, 27, 31].

Ballistic injector formulations balance the physicochemical integrity of the active agent with the mechanical robustness of particles to breach the skin [17, 32–36]. A formulation developed specifically for use with needle-free particle injectors, tested in a successful phase I clinical study with an influenza vaccine, comprised trehalose, mannitol, and dextran (10kDa) at 35% by mass and produced Fluvirin[®]-loaded particles with a 39 μm diameter and a tap density of 0.72 g/cm^3 , yielding a 10.5 kg/ms impact parameter at the devices' estimated exit velocity of 750 m/s [37, 38]. Later work optimized the SFD process parameters for the needle-free injection of glucagon-loaded particles, and added a higher MW dextran 150 kDa to the TMD formulation for increased mechanical robustness. The 35% by mass trehalose-mannitol-dextran_{10kDa}-dextran_{150kDa} (TMDD) excipient matrix achieves the required physical characteristics and enables ballistic injection [27, 31].

Here we report the development of a needle-free TMDD formulation of the meningococcal serogroup Y glycoconjugate MenY-CRM₁₉₇ with suitable physical characteristics for intradermal powder injection using spray-freeze drying. The chemical integrity of MenY-CRM₁₉₇ after SFD was assessed using SDS-PAGE, and its physical integrity by asymmetric flow field-flow fractionation (AF4). An *in vivo* study was conducted and the immune response generated was assayed by ELISA and serum bactericidal assay (SBA). The efficacy of the needle-free formulation was compared to the current clinical standard, MenY-CRM₁₉₇ (plus Alum-adjunct) delivered by intra-muscular injection. This is the first account of needle-free inoculation by dry-powder injection with a complex glycoconjugate vaccine.

Materials and methods

Manufacture of spray-freeze-dried MenY-CRM₁₉₇ powders

The investigational MenY-CRM₁₉₇ vaccine had a polysaccharide-to-protein ratio of 0.625 by mass, contained 3 mg/mL of the meningococcal serogroup Y polysaccharide (Men Y), 4.8 mg/mL *Corynebacterium diphtheriae* CRM₁₉₇ protein, and was suspended in 10% (w/v) sucrose in 10 mM K_2HPO_4 buffer pH 7.2 (provided by Novartis Vaccines and Diagnostics, Siena, Italy). For comparison, the commercial vaccine Menveo[®] (Novartis Vaccines) contains 10 μg Men A polysaccharide and 5 μg of the Men C, Men W and Men Y polysaccharides conjugated to a total of 32 – 64 μg CRM₁₉₇, which corresponds to a polysaccharide-to-protein ratio of 0.39 – 0.78 by mass.

Dry-powder formulations of MenY-CRM₁₉₇ for application in needle-free injection were prepared by a process previously described by Johnson et al. ([39]) and Costantino et al. [28, 29]. Formulations of trehalose, mannitol, dextran (10 kDa), dextran (150 kDa) (3:3:3:1) 35% (w/w) in 10 mM K_2HPO_4 buffer pH 7.2; contained 0.5% wt. MenY-CRM₁₉₇ (mass of MenY-CRM₁₉₇ to

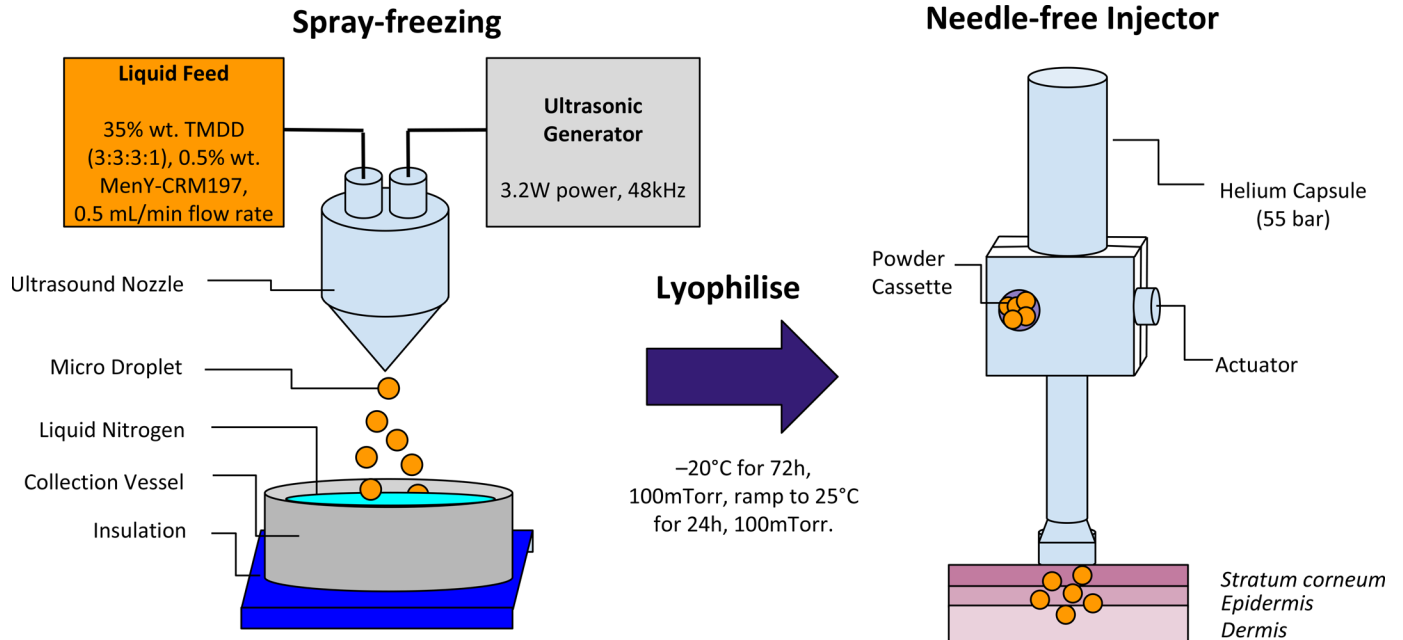


Fig 1. Spray freeze dry process for MenY-CRM₁₉₇ powders. The spray freeze drying set-up used a 48 kHz ultrasound nozzle to atomise the 35% wt. TMDD (3:3:3:1) excipient solution containing 0.5% wt. MenY-CRM₁₉₇, at 3.2W power and a 0.5mL/min flow rate. Particles were shock-frozen into liquid nitrogen and transferred into a pre-equilibrated LyoStar I and lyophilized. The product was filled into injector device powder cassettes, and stored at -80°C until use.

<https://doi.org/10.1371/journal.pone.0183427.g001>

mass of excipients). Stainless steel collection vessels were fitted with precision fine wire thermocouples (Omega Engineering, LTD). Formulations were sprayed into collection vessels filled with liquid nitrogen (Fig 1), using a 48 kHz ultrasound nozzle (Sono-Tek, Milton, NY, USA) at 3.2 W (Broadband Ultrasonic generator, Sono-Tek, NY, USA) and a flow rate of 0.5 mL/min set by a Minipuls3 peristaltic pump (Gilson, Villers Le Bel, France). Once LN₂ had boiled off, the collection vessels were sealed with a Gore Lyoguard lid (W.L. Gore & Associates, Newark, USA). The closed collection vessels were transferred onto pre-cooled shelves (-40°C) and lyophilized in a FTS Systems LyoStar I (SP Industries, Warmister, PA, USA) at 100mTorr and a primary drying temperature of -20°C for 72 h. Secondary drying was conducted at 25°C for 24 h. All SFD formulations were lyophilized above their respective glass transition temperatures T_g' to obtain less porous and more robust particles via viscous flow compaction of the amorphous glass [15]. The powders were transferred from the stainless steel collection vessels into freeze drying vials in a low humidity glove box at RT, sealed, crimped, and frozen to -80°C for storage.

Protein concentration determination by BCA assay

BCA was conducted according to supplier's instructions (Bicinchoninic Assay Kit—Quanti-Pro™ BCA Assay Kit, Sigma Aldrich, UK). Briefly, BCA working reagent was prepared from of a 1:1 dilution of solution QA with QB, and activated with copper (II) sulfate reagent QC in a ratio of 1:50 to QA-QB. CRM₁₉₇ containing samples were added to the working reagent in a 1:1 ratio per well on an optically clear 96-well plate (Corning, UK). CRM₁₉₇ concentration was determined relative to a BSA standard curve with concentrations 0, 0.5, 5, 10, 20, 30 µg/mL made in identical buffer to the samples. The plate was incubated at 37°C for 2h and absorbance was measured on a FLUOstar Omega (BMG Labtech LTD, Aylesbury, UK) plate reader at λ = 562nm. Concentrations were adjusted to blank and related to the BSA concentration curve.

Turbidity measurements

Solution turbidity of ultrasound-atomized excipient solutions containing 2 mg/mL MenY-CRM₁₉₇ was measured on a Varian Cary 50 Bio UV-Visible Spectrophotometer (Varian, Yarton, UK) with a quartz precision cell (Hellma, GER) of 10 mm light path at $\lambda = 500$ nm at RT. Untreated excipient-MenY-CRM₁₉₇ solutions served as control. Turbidity is expressed as the absorbance value at $\lambda = 500$ nm.

Determination of T_g and T_g' for needle-free formulations

Differential scanning calorimetry (DSC) was used to determine the glass transition temperature (T_g) of the dry-powder after SFD. For T_g determination, approximately 5 mg of SFD-powder was weighed, and sealed into the hermetic Tzero aluminium pans (TA Instruments, T111208) and the corresponding aluminium lid (TA Instruments, T1111019). The protocol equilibrated the sample at -10°C and held it isothermal for 20 min. The temperature was ramped to 90°C at $10^{\circ}\text{C}/\text{min}$. Analysis of the thermal signals was performed with TA Universal Analysis 2000 Software (Version 4.7A). The heat capacity thermogram ($\text{J}/\text{g}^{\circ}\text{C}$) was plotted and used for analysis. The temperature at the inflection point of the endothermic shift in heat capacity was reported as the glass transition temperature. For T_g' determination, 20 μL of excipient solution with either 2 mg/mL CRM₁₉₇, or without, was pipetted into hermetic Tzero aluminium pans (TA Instruments, T111208) and hermetically sealed with the corresponding aluminium lid (TA Instruments, T1111019). Samples were analysed on a Q2000 DSC, and computer operated with Thermal Advantage Software interface Version 2.8. Samples were equilibrated at -60°C and held isothermal for 20 min. The temperature was then modulated with $\pm 0.5^{\circ}\text{C}$ every 100 seconds. After 5min isothermal, the temperature modulation had stabilised. The temperature was ramped to 0°C at $1^{\circ}\text{C}/\text{min}$.

Helium-pycnometry and tapped density measurements

The density of powders (ρ_{He}) was measured with a helium pycnometer (Pycnomatic ATC, ThermoFisher, Loughborough, UK). The measurement chamber was fitted with a small volume vessel unit (6.95255 cm^3). The sample chamber volume was further reduced by 3.28743 cm^3 using a unit filler to allow for the accurate density determination of very small powder samples. Density measurements were performed on 0.1–0.5 g of powder. Prior to measurement, the sample chamber was purged with helium for 20 cleaning cycles at 20°C . A total of 5 sample measurements within a maximum error of 1% was used to calculate the reported density. Tap density (ρ_{tap}) was determined according to Method A in document QAS/11.450, published by the WHO in 2012 for addition to the International Pharmacopeia. However, instead of a 250mL volumetric glass cylinder, a converted volumetric 5mL pipette tube was used to measure the small powder samples. The machine used for tapped density determination was built in-house by the IBME workshop. Briefly, a small electronic motor moves a circular brass disc according to a pre-set speed and raises a metal plateau upon which the graded volumetric plastic pipette cylinder is attached. The plateau with the sample containing cylinder is raised about 1cm in height and drops by force of gravity alone, before being raised and dropped again. While the tap height remains constant, the tap frequency can be adjusted based on the supplied voltage to the motor, which alters the rotational speed of the disc. The total number of taps required according to the International Pharmacopeia recommendation before each measurement was divided by the frequency (taps per minute). The thus calculated required time (min) was kept using a stopwatch. From helium pycnometry and tapped density

values, the porosity of particles was calculated according to the equation:

$$\varepsilon = 1 - \frac{\rho_{\text{tap}}}{\rho_{\text{He}}} \quad (1)$$

Powder flowability was calculated using Carr's compressibility index, which relates the free powder bulk density to the tapped bulk density according to the equation:

$$C = 100 \left(1 - \frac{\rho_{\text{bulk}}}{\rho_{\text{tap}}} \right) \quad (2)$$

Particle size analysis with laser light diffraction

Size volume and number distribution of particles were obtained on a Malvern Mastersizer S (Malvern Instruments Ltd, Malvern, UK), in a small volume dispersion cell. A 300RF lens with backscatter detector with an active beam length of 14.3 mm was used to obtain an average of 6 times 6000 measurements according to Mie theory. Particles were added until 10–13% detector obscuration was achieved at 2000 rpm stirring rate. Particles were characterized by median diameter, $D(v, 0.5)$ and span of the volume distribution:

$$\text{Span} = \frac{d(v, 0.9) - d(v, 0.1)}{d(v, 0.5)} \quad (3)$$

$D(v, 0.5)$ corresponds to the median diameter of the volume distribution, and $d(v, 0.1)$ and $d(v, 0.9)$ to the particle diameter at 10% and 90% of the cumulative distribution. Refractive indices for SFD particles (RI 1.5376) in isopropanol (RI 1.3776) were used in the method.

Karl-Fisher Titration- residual moisture determination

A Karl-Fischer DL39 titrator with Stromboli oven and autosampler (Mettler Toledo, Leicester, UK) was used to determine the residual moisture content of 100 mg powder samples. Titration was performed at 125°C for 30 min. Results are reported as %wt. of water relative to the powder mass.

Scanning electron microscopy

The morphology of powder particles was examined on an Amray 1810 T Scanning Electron Microscope (SEM) at 20 kV. The samples were fixed on an aluminium disc (model G 301, Plano) using a carbon adhesive sheet. Samples were gold-sputtered at 20 mA and 5 kV (Hummer JR Technics, Germany) for 1–5 min prior to imaging.

SDS-PAGE

SDS-PAGE used the Hoefer SE250 (Hoefer, Holliston, MA) set-up and a PowerPac (BioRad, Hercules, CA) power unit in combination with a precast 4 – 20% Precise Tris-Glycine gel, 15-Well (Thermo Scientific, Piers Protein Research, USA) and the PrecisionPlus Protein Dual-colour 500 μL (BioRad, USA). Running buffer (5x- concentrated) was prepared from 14.5 g Tris base, 72 g glycine, 5 g SDS in 1 L MilliQ water, and filtered with 0.22 μm Millipore SteriCup. Sample stain comprised of 2 mL 1 M Tris-Cl pH6.8, 6 g glycerol, 1.6 g SDS, 4 mg Brilliant Blue, 0.62 g DTT, for a 20 mL final volume. The staining solution comprised of 0.05% (w/v) Coomassie R Brilliant Blue (CBB), 10% (v/v) acetic acid, 45% (v/v) methanol, 45% (v/v) milliQ water, and the destaining solution of 10% (v/v) acetic acid, 30% (v/v) methanol, 60% (v/v) milliQ water. Sample concentrations ranged between 20 $\mu\text{g}/\text{mL}$ to 300 $\mu\text{g}/\text{mL}$, and 20 μL were used per

well, and 5 μ L of the PrecisionPlus protein ladder (BioRad, UK). Gels were run for 45 min at 185 V. After the run, the SDS-PAGE gel was rinsed in milliQ water for 5 min with 3 complete changes. The gel was stained overnight in a sealed tupperware-box placed on a rocker. Destaining was conducted for 4 hours or until the gel was clear, with at least 2 full changes of destaining solution. The gel was imaged on Gel DocTM XR (BioRad, USA) with Quanti One 4.66 software and analysed in GelAnalyser2010 (Freeware, <http://gelanalyzer.com/>).

Immunisation experiments in mice

Procedures were performed according to the U.K. Animals (Scientific Procedures) Act 1986 and were approved by the University of Oxford Animal Care and Ethical Review Committee. Six to 8-week-old female BALB/c-OlaHsd mice (Harlan, UK) were housed in specific pathogen-free conditions. The vaccine dose per mouse was 8 μ g of CRM with 5 μ g of MenY polysaccharide with or without 85 μ g of Alhydrogel[®] (Alum) (Benntag Biosector, Denmark) as stated in figure legends. The ratio of polysaccharide to protein in the MenY-CRM₁₉₇ vaccine was 0.625. The vaccines were given either intramuscularly (IM) to both hind thigh muscles, intradermally (ID) to the pinna of a single ear or by needle free powder injection to the pinna of a single ear. There was a four-week interval between priming and boosting immunizations. Blood from tail bleeds or terminal cardiac bleeds was collected into Eppendorf tubes at day 28 and day 42 after the priming immunization. Blood was allowed to clot and centrifuged at 15,000 \times g for 10 minutes. Sera were aliquoted and stored at -20° C until use.

Meningococcal serotype Y polysaccharide ELISA

Meningococcal capsular group Y polysaccharide-specific IgG antibodies were measured by ELISA following a previously described method [40]. Briefly, immulon-2 microtiter plates (Thermo Fischer Scientific, MA, USA) were coated with capsular group Y meningococcal polysaccharide (5 μ g/ml) (NIBSC, England) conjugated to 5 μ g/ml of methylated human albumin (NIBSC, England) in sterile PBS. Following blocking, two-fold dilutions of test sera were assayed in duplicate. After overnight incubation at 4° C, microtiter plates were developed with HRP-conjugated goat anti-mouse secondary antibody (Jackson ImmunoResearch Inc. PA, USA) at a 1:10,000 dilution for 2.5 h at room temperature, followed by the chromogenic substrate tetramethylbenzidine (Sigma-Aldrich, England). The reaction was stopped after 30 min with 2 M H₂SO₄. The optical density of each well was read at 450 nm. Endpoint-titres were determined as the reciprocal of the dilution giving an OD_{450 nm} reading above that obtained for naive control wells plus 2 \times SD of 6 replicates for each plate.

Serum bactericidal assay (SBA)

Bactericidal antibody responses were measured using SBA with human complement, as previously described [41]. The SBA was performed on serum from individual mice two weeks after the second dose of MenY-CRM₁₉₇. Exogenous human complement (serum) without intrinsic bactericidal activity was sourced from a consenting healthy adult and used at 25% (vol/vol). Mouse sera were heat inactivated at 56° C for 30 minutes to remove intrinsic complement. The capsule group Y meningococcal strain 860800 Y:P5-1,10-4: F4-1:ST-29 (cc167) was grown overnight on blood agar plates at 37° C with 5% CO₂. Approximately 50 colonies were sub-cultured for 4 hours, and reconstituted in Hanks buffered salt solution (Thermo Fischer Scientific, MA, USA) with 0.5% bovine serum albumin (Sigma Aldrich, MO, USA). The bacteria were diluted to give approximately 100 colony forming units per 10 μ l used for the assay. The

SBA titre was defined as the reciprocal of the highest dilution of serum that yielded $\geq 50\%$ decrease in CFU relative to that of control wells within 60min at 37°C.

Results

Addition of Polysorbate 80 to Trehalose-Mannitol-Dextran10kDa-Dextran150kDa (TMDD) does not reduce aggregation of MenY-CRM₁₉₇ during SFD relative to TMDD alone

Protein aggregates may induce cytotoxicity and misguided antibodies [42]. Therefore, we tested TMDD formulations for visible aggregates of CRM₁₉₇ before and after spray-freeze-drying (SFD) using light scattering ($\lambda = 500$ nm). We investigated whether the addition of the surfactants Polysorbate 80, Polysorbate 20, Poloxamer K188, or Kolliphor HS, at three different concentrations 0.01% wt, 0.1%wt, and 1% wt reduces protein aggregation relative to the standard TMDD (3:3:3:1) matrix. The high surfactant concentration (1% wt.) was excluded from further formulations due to visible foaming during the spray process. Of the tested surfactants at 0.01 and 0.1 wt.%, Polysorbate 80 showed the least CRM₁₉₇ loss during SFD (data not shown). Polysorbate 80 (0.1% wt.) does not reduce protein aggregation during SFD relative to the standard TMDD (3:3:3:1) matrix (Fig 2). MenY-CRM₁₉₇ liquid formulations with 35% (w/w) TMDD (2.6 ± 1.8 mOD₅₀₀) and 35% (w/w) TMDD-PS80 (0.5 ± 0.9 mOD₅₀₀) showed low OD₅₀₀ levels and were not different from one another before and after SFD. After ultrasound atomisation,

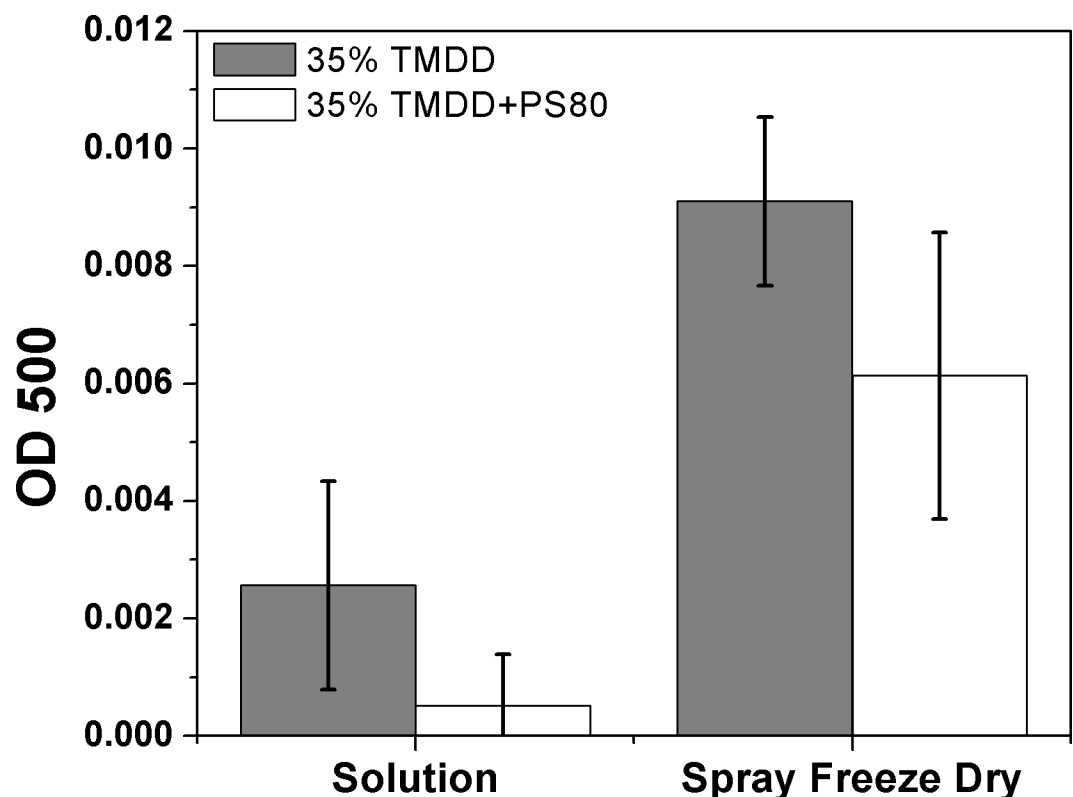


Fig 2. Turbidity measurements (OD₅₀₀) of 2 mg/mL MenY-CRM₁₉₇ a) in solution, and after b) atomisation, freezing and lyophilisation and resuspension. Solutions contained 35% wt (3:3:3:1) trehalose, mannitol, dextran (10kDa), dextran (150kDa), and 35% wt. TMDD with 0.1% (w/w) Polysorbate 80, in 10mM K₂HPO₄ buffer pH 7.2. The addition of PS80 to TMDD did not result in significantly lower turbidity (OD₅₀₀) of the resuspended powder vaccine.

<https://doi.org/10.1371/journal.pone.0183427.g002>

OD₅₀₀ levels increased approximately 3.5-fold for TMDD and 12-fold for TMDD+PS80, and were significantly higher than OD₅₀₀ levels of the initial liquid TMDD (9.1 ± 1.4 mOD₅₀₀) and 35% TMDD-PS80 (6.1 ± 2.4 mOD₅₀₀) formulations. BCA assay indicated a 4% loss of protein after SFD (4.7 ± 0.2 µg/mL) relative to stock solutions (4.9 ± 0.1 µg/mL) for both formulations. To keep the formulation and subsequent analysis simple, 35% (w/w) TMDD (3:3:3:1) without PS80 was used for dry-powder vaccine formulation.

SFD dry-powder formulation creates vaccine-loaded microparticles with sufficient physical robustness for needle-free powder injection

To enable pain-free intradermal delivery, vaccine particles need to breach the *stratum corneum*, which requires a particle impact parameter of 7–12 kg/m·s, a particle size less than 100 µm, and sufficient physical robustness. Lyophilisation of the frozen TMDD droplets above their glass transition temperature ($T_g' = -29.2 \pm 0.4^\circ\text{C}$) produced free-flowing powders that comprised of micron-sized individual particles with the characteristic wrinkled surface morphology (Fig 3). Particles contain 0.5% wt. MenY-CRM₁₉₇ (mass of MenY-CRM₁₉₇ to mass of excipients), unchanged from the pre-SFD suspension.

TMDD and MenY-CRM₁₉₇-TMDD particles had mean diameters of 57.4 µm and 58.1 µm respectively (Table 1). The bulk density of the TMDD particles corresponded to literature values of the sugars, approximately $1.60\text{ g/cm}^3 \pm 1\%$ (Table 1). The tap density of particles was 3.4-fold lower ($0.47 \pm 0.07\text{ g/cm}^3$), which translates to an average particle porosity of 70.6%, with a high glass transition temperature ($T_g = 42.8 \pm 0.5^\circ\text{C}$) and low residual moisture content $0.6 \pm 0.2\%$ (w/w) of the final SFD powder formulation.

The addition of 0.5% (w/w) MenY-CRM₁₉₇ to the 35% (w/w) TMDD (3:3:3:1) matrix changed several physical properties of the particles. The particles were less porous (64.4%) than pure TMDD particles, with a bulk density of $1.49\text{ g/cm}^3 \pm 1\%$ and a 2.8-fold lower tap density ($0.53 \pm 0.09\text{ g/cm}^3$). A higher glass transition temperature ($T_g = 45.2 \pm 0.5^\circ\text{C}$) and a higher residual moisture content $3.5 \pm 1.5\%$ (w/w) were observed. The glass transition temperature ($T_g' = -29.2 \pm 0.4^\circ\text{C}$) was not different from the pure TMDD freeze-concentrate, and therefore the same lyophilisation program was used.

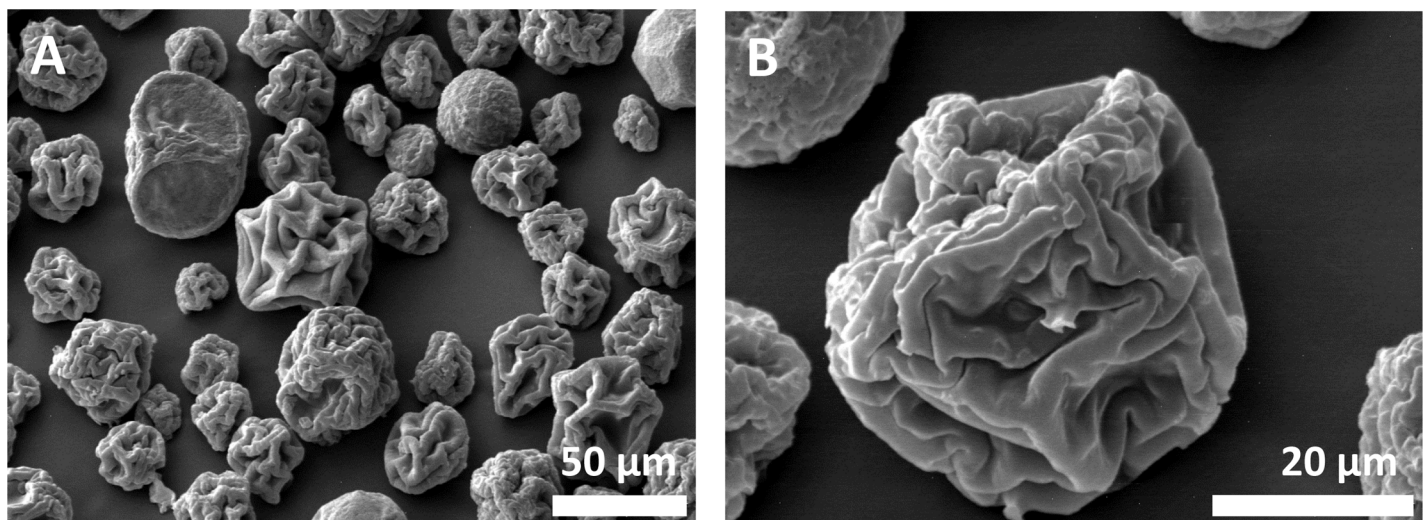


Fig 3. Microparticle size distribution (A) and surface morphology (B) by SEM. Microparticles with average diameter of 58.1 µm were produced by SFD from a 35% (w/w) TMDD-MenY-CRM₁₉₇ (3:3:3:1) solution, lyophilized at -20°C and 100 mTorr (0.13 mbar) for 72 hours (primary drying) and at 20°C and 100 mTorr for 24 hour (secondary drying,) show a wrinkled surface morphology characteristic of trehalose-manitol-dextran particles.

<https://doi.org/10.1371/journal.pone.0183427.g003>

Table 1. Physical characteristics of matrix and vaccine SFD formulations.

Formulation property	TMDD	TMDD-MenY-CRM ₁₉₇
Solid Content (% wt.)	35	35
TMDD Relative Ratio	3:3:3:1	3:3:3:1
MenY-CRM content (% wt.)	0.0	0.5
1 ^o Drying (°C, mTorr, hrs)	-20, 100, 72	-20, 100, 72
2 ^o Drying (°C, mTorr, hrs)	20, 100, 24	20, 100, 24
Yield (% wt. solutes/powder)	92 ± 7%	90 ± 8%
Residual H ₂ O (% wt.)	0.6 ± 0.2	3.5 ± 1.5
Tg' (°C)	-29.2 ± 0.4	-29.9 ± 0.3
Tg (°C)	42.8 ± 0.5	45.2 ± 0.5
dCp (J/g°C)	0.69 ± 0.01	0.45 ± 0.03
D(v, 0.5) (µm), (Span)	57.4 (1.3)	58.1 (1.2)
He-Pycnometry (g/cm ³)	1.60 ± 1%	1.49 ± 1%
Tapped Density (g/cm ³)	0.47 ± 0.07	0.53 ± 0.09
Carr's Index	11.3 ± 0.8	15.7 ± 1.4
Porosity (%)	70.6	64.4
Impact Parameter (pv _r)	10.1	11.5

<https://doi.org/10.1371/journal.pone.0183427.t001>

The observed particle diameters and the calculated impact factors for TMDD (10.1 kg/m·s) and TMDD-CRM₁₉₇ (11.5 kg/m·s) fall within the recommended range for pain-free intradermal powder injection [16, 20].

Chemico-physical integrity of MenY-CRM₁₉₇ is maintained during SFD

Aggregation of biotherapeutic proteins has been linked to cytotoxicity, decreased biological activity, and increased immunogenicity. According to SDS-PAGE, the 58.4 kDa [43] CRM₁₉₇ protein control showed a defined band at 60 kDa (Fig 4). The untreated control MenY-CRM₁₉₇ and resuspended dry-powder MenY-CRM₁₉₇-TMDD bands appear equivalent to each other, without detectable hydrolysis products in the lower MW band region. Detectable fractions ranged from 300 kDa to 75 kDa (Table 2). The wide range of MenY-CRM₁₉₇ molecular weights (band smear) in the stock and post-SFD lanes arises from heterogeneous MenY polysaccharide substitution to the CRM₁₉₇ carrier protein [44, 45]. Asymmetric flow field-flow fractionation of the MenY-CRM₁₉₇ vaccine before and after SFD showed a 93% ± 6% recovery of MenY-CRM₁₉₇, and did not detect physical aggregates (see Figure A S1 File). The total protein mass detected in the band intensities correspond to the nominal values (12ng MenY-CRM₁₉₇), as calculated by the integration of the intensity bands relative to a CRM₁₉₇ standard curve.

Delivery of MenY-CRM₁₉₇ vaccine by powder injection induces MenY-polysaccharide specific antibodies

Having established that the SFD process could produce particulates with the desired characteristics without impacting on the immunogen structure, we sought to compare the humoral response in Balb/C mice after administration of a MenY-CRM₁₉₇ vaccine using a needle free powder injector (NFPI), to intradermal (ID) or intramuscular (IM) delivery. Two doses of MenY-CRM₁₉₇ were given to groups of mice with a four-week interval. The ID and IM vaccines were formulated with or without Alhydrogel (Alum) although the MenACWY-CRM vaccine (Menveo, GSK) is not adjuvanted but the use of Alum in our experiments would

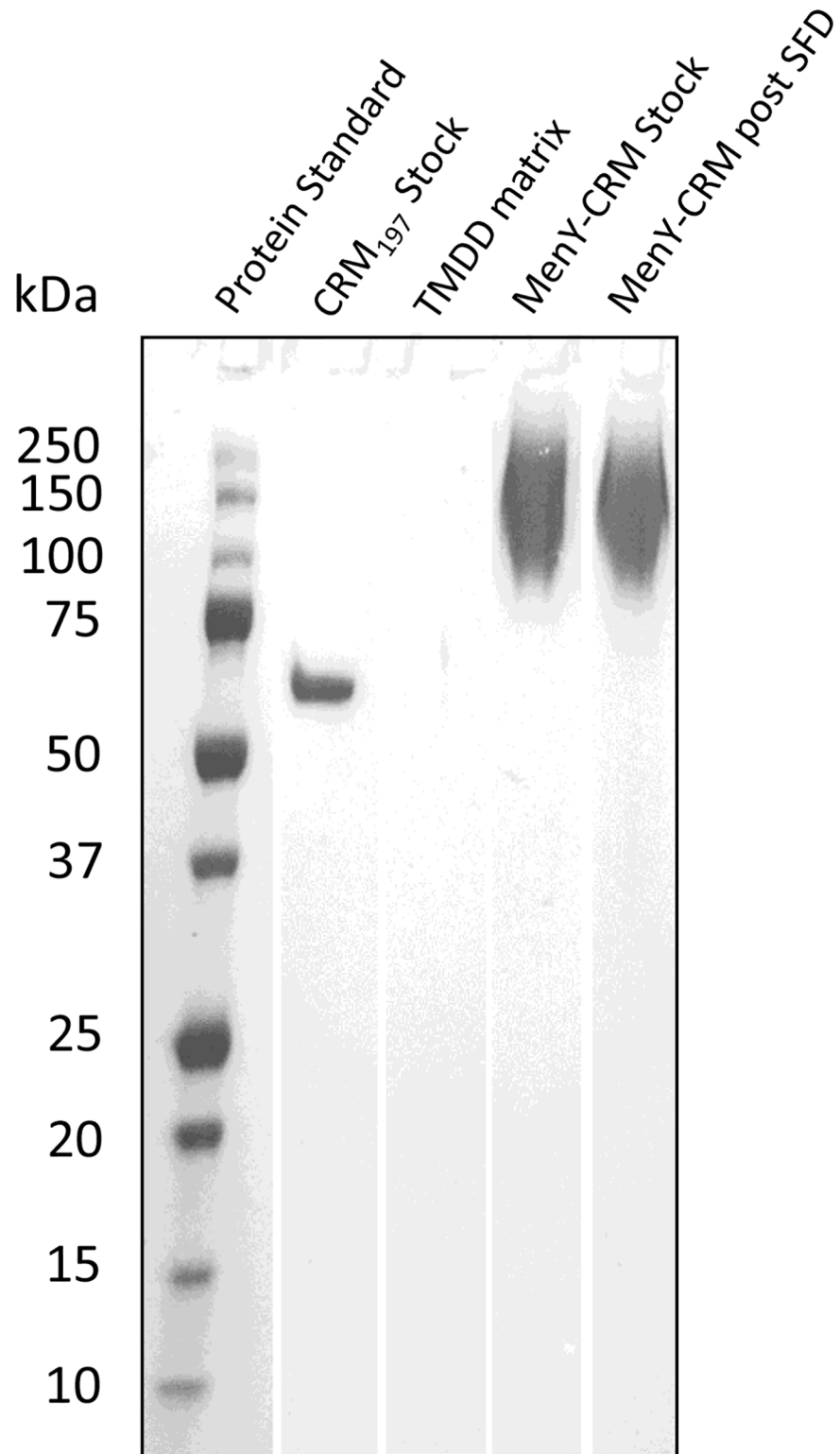


Fig 4. Chemico-physical integrity of MenY-CRM₁₉₇ assessment by SDS-PAGE. SDS-PAGE used precast 4–20% Precise Tris-Glycine gels and the PrecisionPlus Protein Dual-colour protein standard. Samples were applied to the 15-well gel in every other lane. Control lanes were loaded with CRM₁₉₇ stock protein (2.0 ng), 35% (w/w) TMDD matrix without MenY-CRM₁₉₇ (10 µg), untreated MenY-CRM₁₉₇ stock (12 ng), and resuspended SFD MenY-CRM₁₉₇ (12 ng) SFD powder.

<https://doi.org/10.1371/journal.pone.0183427.g004>

Table 2. Semi-quantitative size analysis of MenY-CRM₁₉₇ by SDS-PAGE.

SDS-PAGE analysis	CRM ₁₉₇ Stock	MenY-CRM ₁₉₇ Stock	MenY-CRM ₁₉₇ Post SFD
Total mass (µg) in lane (vs. nominal)	2.2 (2.0)	11.9 (12.0)	11.6 (12.0)
Upper bound (kDa)	66	1790	1590
Median (kDa)	62	150	149
Lower bound (kDa)	58	77	74
Aggregates (%)	ND	ND	ND
Hydrolysis products	ND	ND	ND

<https://doi.org/10.1371/journal.pone.0183427.t002>

provide a more rigorous comparison. ELISAs were performed to determine the titres of MenY-polysaccharide specific IgG antibodies for each of the different groups after two doses of the vaccine (Fig 5B). All groups had measurable antibody responses but one mouse out of 6 in the MenY-CRM₁₉₇ NFPI group had an antibody level below the limit of detection (equivalent to naïve mice). Mice in the MenY-CRM₁₉₇ IM + Alum group had the greatest geometric mean antibody titre (26257, 95% CI 15714, 43872), which was significantly greater ($P < 0.01$) than that of the MenY-CRM₁₉₇ ID group (449, 95% CI 94, 2125) and the MenY-CRM₁₉₇ NFPI group (566, 95% CI 117, 2739). All other comparisons between the MenY-CRM₁₉₇ IM and MenY-CRM₁₉₇ ID + Alum groups (1796, 95% CI 332.9, 9688 and 9051, 95% CI 3320, 24673 respectively) were not significant ($P > 0.05$).

Pooled sera from mice in the MenY-CRM₁₉₇ IM + Alum and the MenY-CRM₁₉₇ NFPI groups were used to perform IgG1, IgG2a, IgG2b and IgG3 subclass ELISAs against MenY polysaccharide. This was to investigate whether there was a difference in the subclasses induced by the different routes of vaccine administration. The responses were very weak or undetectable for all of the subclasses (data not shown) with the exception of IgG1 where the OD450nm reading was 2.8 for the MenY-CRM₁₉₇ IM + Alum group compared with OD450nm = 0.5 for the MenY-CRM₁₉₇ NFPI group, both at a serum dilution of 1/250 (data not shown).

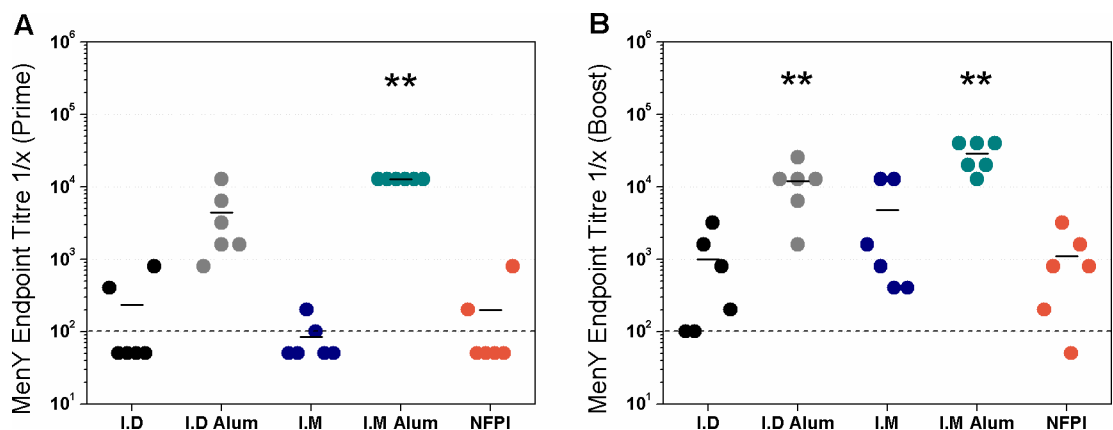


Fig 5. MenY polysaccharide-specific IgG responses to MenY-CRM₁₉₇ prime (A) and boost (B) administered IM, ID or by needle free powder injection. Total IgG end-point titres in Balb/c mice were measured by MenY-polysaccharide ELISA after two 5µg doses of MenY-CRM₁₉₇ delivered either ID, IM or by needle free powder injection on days 28 and 42. ID and IM vaccinations were performed with or without Alum as indicated on the X axis. The geometric mean values for each group are indicated by bars. The limit of detection is indicated by the dashed line. n = 6 per group. ** = $P < 0.01$ by Kruskal-Wallis with Dunns post-test compared with pooled sera of naïve mice. Values below 100 were designated an arbitrary value of 50.

<https://doi.org/10.1371/journal.pone.0183427.g005>

Vaccination by needle free powder injector results in comparable serum bactericidal antibody titres with ID and IM MenY-CRM197 vaccine delivery

Due to low incidence rates of meningococcal disease globally, efficacy trials of new vaccines are unfeasible. Therefore, meningococcal vaccines are licensed based upon a surrogate of protection, which is a serum bactericidal antibody (SBA) titre $\geq 1:8$ when using rabbit complement (rSBA) or $\geq 1:4$ when using exogenous human complement (hSBA). We therefore measured the bactericidal antibody responses after ID, IM or needle free powder injection administration of the MenY-CRM₁₉₇ vaccine in the same experimental groups of mice used to perform the ELISAs (Fig 6). After two doses of vaccine the geometric mean hSBA titres in the MenY-CRM₁₉₇ ID and MenY-CRM₁₉₇ IM groups (both without Alum) (57.0, 95% CI 4.0, 815.0 and 6.4, 95% CI 0.7, 56.8 respectively) were not significantly greater than that of the naïve group (2.3, 95% CI 0.2, 23.1), which contained an outlier hSBA titre of 1:64 in one animal. The MenY-CRM₁₉₇ NFPI and MenY-CRM₁₉₇ ID + Alum groups had significantly ($P < 0.05$) greater geometric mean hSBA titres (228.1, 95% CI 60.0, 866.6 and 287.4, 95% CI 140.5, 587.6 respectively) compared with the naïve group. None of the groups that received the vaccine by a traditional injection route had a greater mean hSBA titre than the MenY-CRM₁₉₇ NFPI group.

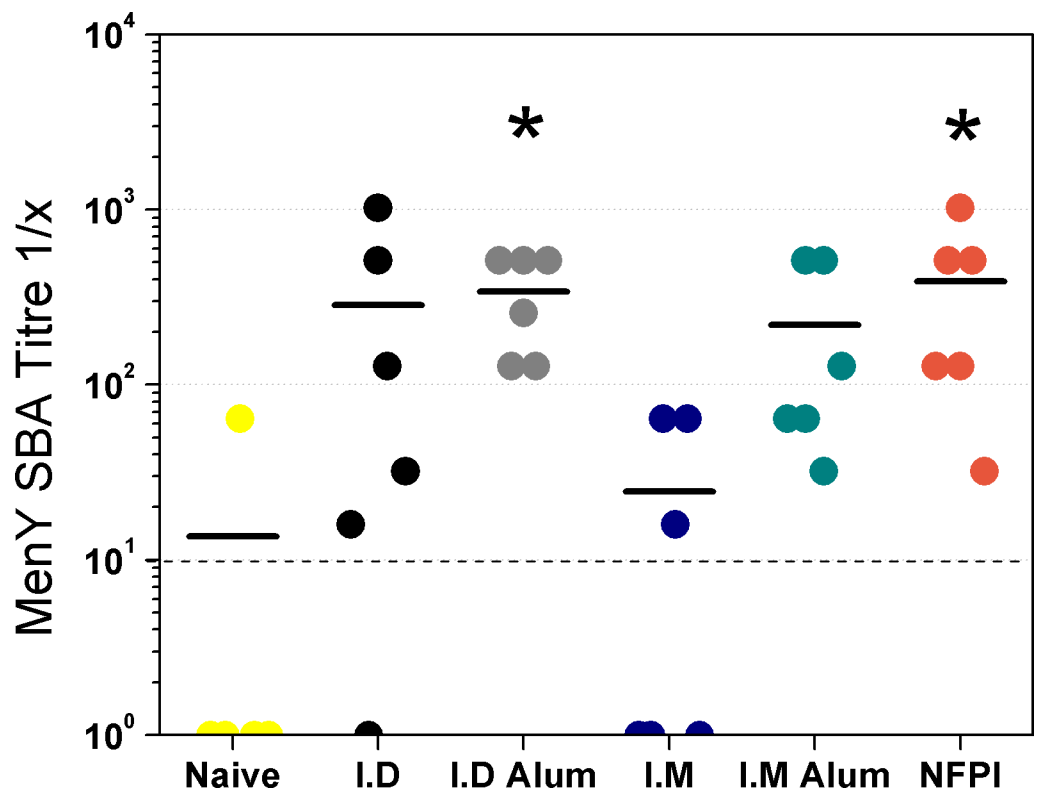


Fig 6. Serum bactericidal antibody responses to MenY-CRM₁₉₇ administered IM, ID or by needle free powder injector. hSBA end-point titres in Balb/c mice were measured after two 5µg doses of MenY-CRM₁₉₇ delivered either ID, IM or by needle free powder injector (NDPI). ID and IM vaccinations were performed with or without Alum indicated in the axis. The geometric means for each group are indicated by bars. The limit of detection is indicated by the dashed line. n = five or six per group. * = $P < 0.05$ by Kruskal-Wallis with Dunns post-test compared with Naïve group. SBA titres below 1:4 were designated an arbitrary value of 1.

<https://doi.org/10.1371/journal.pone.0183427.g006>

Discussion

In this study we have shown that delivery of the MenY-CRM₁₉₇ vaccine by needle free powder injection results in bactericidal antibody responses that are comparable with alum-adjuvanted ID or IM vaccinations in mice. We have also shown that spray-freeze drying a high solute content TMDD-MenY-CRM₁₉₇ solution produces vaccine-loaded microparticles with suitable physical characteristics for NFPI that adequately preserve MenY-CRM₁₉₇ structure.

To reduce the effect of the shear stress and possible hydrophobic patch association of CRM₁₉₇ molecules at interfaces created during atomisation, Polysorbate80, a pharmaceutical grade surfactant was used. Relative to TMDD alone, the addition of surfactant showed no significant reduction in MenY-CRM₁₉₇ loss during SFD. This is surprising in that surfactants have been shown to improve the viability of proteins during spray drying and spray-freeze drying [46, 47]. A frequently referenced mechanism of protein preservation by surfactants is their preferential accumulation at solution interfaces which can prevent protein molecules from accumulating and interacting at these interfaces [48]. These findings therefore suggest that intermolecular interactions at interfaces are not the only factor in MenY-CRM₁₉₇ aggregation during atomisation. In addition to shear at the nozzle tip and the subsequent solution-air interface of the droplets, localised heating and high pressures due to cavitation at the ultrasound nozzle tip may lead to protein aggregation. The choice of excipients will need to balance the physico-chemical integrity of MenY-CRM₁₉₇ with the physical requirements for the NFPI microparticles.

While sucrose and trehalose are excellent glass formers and lyo- and cryoprotectants that could preserve MenY-CRM₁₉₇ in a dry matrix, the addition of a plasticiser is necessary to achieve the minimum mechanical robustness required for ballistic injection. Mannitol has been shown to induce substantial viscous flow compaction during freeze-drying [15, 27, 31]. The viscosity of an amorphous matrix decreases significantly at temperatures that exceed its Tg'. This behaviour is described by the Williams-Landel-Ferry equation and is a function of the difference between the product temperature (T_{prod}) and Tg' [49]. Plastic flow occurs usually between the Tg' of a matrix and its collapse temperature (Tc). The collapse of an amorphous freeze concentrate occurs usually at a temperature (Tc) 2°C above its Tg'. Tang and Pikal report that plastic flow may occur when T_{prod} exceeds Tg' or even Tc during primary drying [50]. The T_{prod} of TMDD-CRM₁₉₇ and TMDD exceeded Tg' during 1° drying, and the substantially reduced viscosity can cause matrix deformations by plastic flow and collapse [51]. SEM images show a wrinkled and collapsed morphology. Therefore, TMDD with and without MenY-CRM₁₉₇, are likely compacted via plastic flow during 1° drying, which was conducted above the Tg'. Structural collapse in conventional lyophilisates would see them eliminated from further use, but in case of ballistic delivery, collapse is desirable since it increases the impact parameter. While all examined dextran-containing formulations resulted in powders physically suitable for NFPI after SFD, their ability to preserve MenY-CRM₁₉₇ needed to be investigated.

The molecular weight distribution of a glycoconjugate is a reasonable proxy to inform vaccine immunogenicity. A decrease in immunogenicity was observed only for high degrees of physicochemical degradation of the MenC-CRM₁₉₇, above a 30% loss of the conjugated polysaccharide, and a CRM₁₉₇ aggregate content of 23% [52]. On average, MenY-CRM₁₉₇ has 5 – 10 MenY polysaccharide chains per CRM₁₉₇ monomer (58.4 kDa), each with an average degree of polymerization of 20 – 21, and an average formulation weight of 145 kDa, suggesting an average aggregate MenY content of 87 kDa per glycoconjugate molecule [43]. The presented SDS-PAGE data are in good agreement with published values and range from 75 kDa to 300 kDa, with a mean of 150 kDa. The MenY-CRM₁₉₇ intensity bands by SDS-PAGE and

AF4 elution profile suggest a similar MW distribution before and after SFD. Furthermore, the absence of lower MW bands indicates that the chemical degradation of the CRM₁₉₇ protein after SFD was less than 1%, which is based on the assay's 0.1 µg/band detection limit. Therefore, the chemical integrity of MenY-CRM₁₉₇ was largely preserved during SFD.

Considering the ELISA data, there was no significant effect of the adjuvant Alhydrogel on the antibody end-point titres when the vaccine was delivered either ID or IM. This is in agreement with the finding that in infant studies, decreased immunogenicity in response to the quadrivalent MenACWY-CRM was not observed when aluminium phosphate adjuvant was omitted from the vaccine [53, 54]. However, the ELISA data indicated that mice in the MenY-CRM₁₉₇ IM + Alum group developed the greatest amount of antibodies in response to the vaccine. By comparison, mice in the MenY-CRM₁₉₇ NFPI group appeared to have weaker antibody responses.

The ELISA data are in stark contrast to the results seen in the hSBA. Only groups of mice that received the vaccine by needle-free powder injection or intradermally with Alum developed bactericidal antibody titres that were significantly higher than the naïve group. The discordance between the IgG titres measured by ELISA and the bactericidal antibody titres measured by hSBA are not wholly unexpected. A number of studies have shown that antibodies measured by standard polysaccharide ELISAs do not correlate well with SBA titres [55–58]. This effect has been attributed to differences in the avidity of antibodies, since high avidity antibodies are necessary to induce complement mediated bacterial lysis in the SBA. It has been shown that avidity ELISAs have a stronger correlation with SBA compared with standard ELISA [57]. It is reasonable therefore, that the needle-free powder injector induced fewer antibodies than IM delivery with Alum, but those antibodies were of higher avidity, and resultant, were more bactericidal.

The different routes of vaccine administration could have resulted in different IgG subclasses to be induced. In mice, IgG1 is known to be the main bactericidal subclass produced in response to protein-conjugated polysaccharide vaccines [59]. The only subclass detected was IgG1 which was present in the serum from the MenY-CRM₁₉₇ IM + Alum and the MenY-CRM₁₉₇ NFPI groups. Therefore, it does not appear that the bactericidal antibodies induced by needle-free powder injection were of a different subclass than those induced by IM vaccination. Mice that received the vaccine by ID injection to the ear had similar humoral responses to those that received the vaccine by the powder injector. There is evidence that ID vaccination generally results in stronger immune responses compared with IM vaccination [60–62]. The most likely explanation for this is that the dermis contains a greater proportion of antigen presenting cells such as Langerhans cells, which take up antigens and migrate to lymph nodes where they present their bound antigen to T and B cells [24]. This study shows that needle free powder injection of the MenY-CRM₁₉₇ conjugate vaccine results in bactericidal antibody responses in mice that are equivalent to ID and IM delivery.

The struggle to prevent disease globally is perpetual. While much progress has been made, vaccines and delivery strategies can be improved further. Needle-free intradermal immunisation may expand the medical arsenal that is used to combat infectious diseases. Our results with MenY-CRM₁₉₇ demonstrate that needle free vaccination is both technically and immunologically valid, and could be considered for a broader range of glycoconjugate vaccines in development.

Supporting information

S1 File. AF4 analysis at OD 280nm compared the controls CRM₁₉₇ (10ug), MenY-CRM₁₉₇ stock solution (10ug), versus the resuspended SFD powders containing MenY-CRM₁₉₇. (DOCX)

Acknowledgments

We thank GSK Vaccines (formerly Novartis Vaccines and Diagnostics) for providing the MenY-CRM197 free of charge, Particle Therapeutics Ltd. for providing the injection device and helium cylinders free of charge. We thank Dr. Felix Wolf for assistance with SEM, and Mr. James Fisk and Mr. David Salisbury from the IBME workshop for engineering the SFD set-up and tapped-density device.

Author Contributions

Conceptualization: Nikolas T. Weissmueller, Leanne Marsay, Heiko A. Schiffter, Andrew J. Pollard.

Data curation: Nikolas T. Weissmueller, Leanne Marsay.

Formal analysis: Nikolas T. Weissmueller, Leanne Marsay.

Funding acquisition: Heiko A. Schiffter, Christine S. Rollier, Andrew J. Pollard.

Investigation: Nikolas T. Weissmueller, Leanne Marsay, Christine S. Rollier.

Methodology: Nikolas T. Weissmueller, Leanne Marsay, Heiko A. Schiffter.

Resources: Robert K. Prud'homme, Andrew J. Pollard.

Supervision: Heiko A. Schiffter, Robert C. Carlisle, Christine S. Rollier, Robert K. Prud'homme, Andrew J. Pollard.

Visualization: Nikolas T. Weissmueller, Leanne Marsay.

Writing – original draft: Nikolas T. Weissmueller, Leanne Marsay.

Writing – review & editing: Nikolas T. Weissmueller, Heiko A. Schiffter, Robert C. Carlisle, Robert K. Prud'homme, Andrew J. Pollard.

References

1. World Health Organization. Safety of Injections: Global Facts&Figures. Geneva: World Health Organization, 2004.
2. Wilburn SQ, Eijkemans G. Preventing needlestick injuries among healthcare workers: A WHO-ICN collaboration. *International Journal of Occupational and Environmental Health*. 2004; 10(4):451–6. <https://doi.org/10.1179/oeh.2004.10.4.451> PMID: 15702761
3. Levine MM. Can needle-free administration of vaccines become the norm in global immunization? *Nature Medicine*. 2003; 9(1):99–103. <https://doi.org/10.1038/nm0103-99> PMID: 12514720
4. Mvundura M, Lorenson K, Chweya A, Kigadye R, Bartholomew K, Makame M, et al. Estimating the costs of the vaccine supply chain and service delivery for selected districts in Kenya and Tanzania. *Vaccine*. 2015; 33(23):2697–703. <https://doi.org/10.1016/j.vaccine.2015.03.084> PMID: 25865467.
5. De Gregorio E, Rappuoli R. From empiricism to rational design: a personal perspective of the evolution of vaccine development. *Nat Rev Immunol*. 2014; 14(7):505–14. <https://doi.org/10.1038/nri3694> PMID: 24925139.
6. Blanchard-Rohner G, Pollard AJ. Long-term protection after immunization with protein-polysaccharide conjugate vaccines in infancy. *Expert Rev Vaccines*. 2011; 10(5):673–84. <https://doi.org/10.1586/erv.11.14> PMID: 21604987
7. Kelly DF, Moxon ER, Pollard AJ. Haemophilus influenzae type b conjugate vaccines. *Immunology*. 2004; 113(2):163–74. <https://doi.org/10.1111/j.1365-2567.2004.01971.x> PMID: 15379976
8. Pollard AJ, Perrett KP, Beverley PC. Maintaining protection against invasive bacteria with protein-polysaccharide conjugate vaccines. *Nature Reviews Immunology*. 2009; 9(3):213–20. <https://doi.org/10.1038/nri2494> PMID: 19214194
9. Jafri RZ, Ali A, Messonnier NE, Tevi-Benissan C, Durrheim D, Eskola J, et al. Global epidemiology of invasive meningococcal disease. *Popul Health Metr*. 2013; 11(1):17. <https://doi.org/10.1186/1478-7954-11-17> PMID: 24016339; PubMed Central PMCID: PMC3848799.

10. Arora A, Prausnitz MR, Mitragotri S. Micro-scale devices for transdermal drug delivery. *International Journal of Pharmaceutics*. 2008; 364(2):227–36. <https://doi.org/10.1016/j.ijpharm.2008.08.032> PMID: 18805472
11. Karande P, Jain A, Mitragotri S. Discovery of transdermal penetration enhancers by high-throughput screening. *Nat Biotechnol*. 2004; 22(2):192–7. <https://doi.org/10.1038/nbt928> PMID: 14704682
12. Mitragotri S. Immunization without needles. *Nature Reviews Immunology*. 2005; 5(12):905–16. <https://doi.org/10.1038/nri1728> PMID: 16239901
13. Ogura M, Paliwal S, Mitragotri S. Low-frequency sonophoresis: current status and future prospects. *Adv Drug Deliv Rev*. 2008; 60(10):1218–23. <https://doi.org/10.1016/j.addr.2008.03.006> PMID: 18450318
14. Maa YF, Ameri M, Shu C, Payne LG, Chen D. Influenza vaccine powder formulation development: Spray-freeze-drying and stability evaluation. *Journal of Pharmaceutical Sciences*. 2004; 93(7):1912–23. <https://doi.org/10.1002/jps.20104> PMID: 15176078
15. Sonner C, Maa YF, Lee G. Spray-freeze-drying for protein powder preparation: Particle characterization and a case study with trypsinogen stability. *Journal of Pharmaceutical Sciences*. 2002; 91(10):2122–39. <https://doi.org/10.1002/jps.10204> PMID: 12226840
16. Burkoth TL, Bellhouse BJ, Hewson G, Longridge DJ, Muddle AG, Sarpie DF. Transdermal and transmucosal powdered drug delivery. *Critical Reviews in Therapeutic Drug Carrier Systems*. 1999; 16(4):331–84. PMID: 10532199
17. Chen D, Endres RL, Erickson CA, Weis KF, McGregor MW, Kawaoka Y, et al. Epidermal immunization by a needle-free powder delivery technology: Immunogenicity of influenza vaccine and protection in mice. *Nature Medicine*. 2000; 6(10):1187–90. <https://doi.org/10.1038/80538> PMID: 11017153
18. Kendall M, Mitchell T, Wrighton-Smith P. Intradermal ballistic delivery of micro-particles into excised human skin for pharmaceutical applications. *Journal of Biomechanics*. 2004; 37(11):1733–41. <https://doi.org/10.1016/j.jbiomech.2004.01.032> PMID: 15388316
19. Liu Y. Utilization of the venturi effect to introduce micro-particles for epidermal vaccination. *Medical Engineering and Physics*. 2007; 29(3):390–7. <https://doi.org/10.1016/j.medengphy.2006.05.015> PMID: 16843696
20. Kendall MA. The delivery of particulate vaccines and drugs to human skin with a practical, hand-held shock tube-based system. *Shock Waves*. 2002; 12(1):23–30.
21. Dean HJ, Fuller D, Osorio JE. Powder and particle-mediated approaches for delivery of DNA and protein vaccines into the epidermis. *Comparative Immunology, Microbiology and Infectious Diseases*. 2003; 26(5–6):373–88. [https://doi.org/10.1016/S0147-9571\(03\)00021-3](https://doi.org/10.1016/S0147-9571(03)00021-3) PMID: 12818623
22. Bal SM, Ding Z, Van Riet E, Jiskoot W, Bouwstra JA. Advances in transcutaneous vaccine delivery: Do all ways lead to Rome? *Journal of Controlled Release*. 2010; 148(3):266–82. <https://doi.org/10.1016/j.jconrel.2010.09.018> PMID: 20869998
23. Kupper TS, Fuhlbrigge RC. Immune surveillance in the skin: Mechanisms and clinical consequences. *Nature Reviews Immunology*. 2004; 4(3):211–22. <https://doi.org/10.1038/nri1310> PMID: 15039758
24. Weissmueller NT, Schiffter HA, Pollard AJ. Intradermal powder immunization with protein-containing vaccines. *Expert Rev Vaccines*. 2013; 12(6):687–702. <https://doi.org/10.1586/erv.13.48> PMID: 23750797.
25. Nail SL, Jiang S, Chongprasert S, Knopp SA. Fundamentals of Freeze-Drying. In: Nail SL, Akers MJ, editors. *Development and Manufacture of Protein Pharmaceuticals*. Boston, MA: Springer US; 2002. p. 281–360.
26. Maury M, Murphy K, Kumar S, Shi L, Lee G. Effects of process variables on the powder yield of spray-dried trehalose on a laboratory spray-dryer. *Euro J Pharm Biopharm*. 2005; 59:565–73.
27. Schiffter H, Condliffe J, Vonhoff S. Spray-freeze-drying of nanosuspensions: The manufacture of insulin particles for needle-free ballistic powder delivery. *Journal of the Royal Society Interface*. 2010; 7(SUPPL. 4):S483–S500.
28. Costantino HR, Firouzabadian L, Chichih W, Carrasquillo KG, Griebenow K, Zale SE, et al. Protein spray freeze drying. 2. Effect of formulation variables on particle size and stability. *Journal of Pharmaceutical Sciences*. 2002; 91(2):388–95. PMID: 11835198
29. Costantino HR, Firouzabadian L, Hogeland K, Wu C, Beganski C, Carrasquillo KG, et al. Protein spray-freeze drying. Effect of atomization conditions on particle size and stability. *Pharmaceutical Research*. 2000; 17(11):1374–83. PMID: 11205730
30. Schiffter H. Spray-freeze-drying in the manufacture of pharmaceuticals. *Eur Pharm Rev*. 2007; 12:67–71.

31. Rochelle C, Lee G. Dextran or hydroxyethyl starch in spray-freeze-dried trehalose/mannitol microparticles intended as ballistic particulate carriers for proteins. *J Pharm Sci*. 2007; 96(9):2296–309. <https://doi.org/10.1002/jps.20861> PMID: 17274046.
32. Chen D, Burger M, Chu Q, Endres R, Zuleger C, Dean H, et al. Epidermal powder immunization: Cellular and molecular mechanisms for enhancing vaccine immunogenicity. *Virus Research*. 2004; 103(1–2):147–53. <https://doi.org/10.1016/j.virusres.2004.02.027> PMID: 15163503
33. Chen D, Maa YF, Haynes JR. Needle-free epidermal powder immunization. *Expert Review of Vaccines*. 2002; 1(3):265–76. <https://doi.org/10.1586/14760584.1.3.265> PMID: 12901567
34. Kendall M, Rishworth S, Carter F, Mitchell T. Effects of relative humidity and ambient temperature on the ballistic delivery of micro-particles to excised porcine skin. *Journal of Investigative Dermatology*. 2004; 122(3):739–46. <https://doi.org/10.1111/j.0022-202X.2004.22320.x> PMID: 15086561
35. Maa YF, Shu C, Ameri M, Zuleger C, Che J, Osorio JE, et al. Optimization of an alum-adsorbed vaccine powder formulation for epidermal powder immunization. *Pharmaceutical Research*. 2003; 20(7):969–77. PMID: 12880281
36. Weissmueller NT, Schiffter HA, Carlisle RC, Rollier CS, Pollard AJ. Needle-Free Dermal Delivery of a Diphtheria Toxin CRM197 Mutant on Potassium-Doped Hydroxyapatite Microparticles. *Clin Vaccine Immunol*. 2015; 22(5):586–92. <https://doi.org/10.1128/CVI.00121-15> PMID: 25809632; PubMed Central PMCID: PMC4412946.
37. Chen D, Endres R, Maa YF, Kensil CR, Whitaker-Dowling P, Trichel A, et al. Epidermal powder immunization of mice and monkeys with an influenza vaccine. *Vaccine*. 2003; 21(21–22):2830–6. PMID: 12798624
38. Dean HJ, Chen D. Epidermal powder immunization against influenza. *Vaccine*. 2004; 23(5):681–6. <https://doi.org/10.1016/j.vaccine.2004.06.041> PMID: 15542190
39. Johnson KA. Preparation of peptide and protein powders for inhalation. *Advanced Drug Delivery Reviews*. 1997; 26(1):3–15. PMID: 10837528
40. Gheesling LL, Carlone GM, Pais LB, Holder PF, Maslanka SE, Plikaytis BD, et al. Multicenter comparison of *Neisseria meningitidis* serogroup C anti-capsular polysaccharide antibody levels measured by a standardized enzyme-linked immunosorbent assay. *J Clin Microbiol*. 1994; 32(6):1475–82. PMID: 8077392; PubMed Central PMCID: PMC264022.
41. Borrow R, Carlone GM, Rosenstein N, Blake M, Feavers I, Martin D, et al. *Neisseria meningitidis* group B correlates of protection and assay standardization—international meeting report Emory University, Atlanta, Georgia, United States, 16–17 March 2005. *Vaccine*. 2006; 24(24):5093–107. PMID: 16838413.
42. Ratanji KD, Derrick JP, Dearman RJ, Kimber I. Immunogenicity of therapeutic proteins: influence of aggregation. *J Immunotoxicol*. 2014; 11(2):99–109. <https://doi.org/10.3109/1547691X.2013.821564> PMID: 23919460; PubMed Central PMCID: PMC4002659.
43. Berti F, Costantino P, Fragai M, Luchinat C. Water accessibility, aggregation, and motional features of polysaccharide-protein conjugate vaccines. *Biophys J*. 2004; 86(1 Pt 1):3–9. [https://doi.org/10.1016/S0006-3495\(04\)74078-3](https://doi.org/10.1016/S0006-3495(04)74078-3) PMID: 14695244; PubMed Central PMCID: PMC1303793.
44. Moginger U, Resemann A, Martin CE, Parameswarappa S, Govindan S, Wamhoff EC, et al. Cross Reactive Material 197 glycoconjugate vaccines contain privileged conjugation sites. *Sci Rep*. 2016; 6:20488. <https://doi.org/10.1038/srep20488> PMID: 26841683; PubMed Central PMCID: PMC4740906.
45. Broker M, Berti F, Costantino P. Factors contributing to the immunogenicity of meningococcal conjugate vaccines. *Hum Vaccin Immunother*. 2016; 12(7):1808–24. <https://doi.org/10.1080/21645515.2016.1153206> PMID: 26934310; PubMed Central PMCID: PMC4964817.
46. Wang W. Lyophilization and development of solid protein pharmaceuticals. *International Journal of Pharmaceutics*. 2000; 203(1–2):1–60. PMID: 10967427
47. Wang W. Protein aggregation and its inhibition in biopharmaceutics. *International Journal of Pharmaceutics*. 2005; 289(1–2):1–30. <https://doi.org/10.1016/j.ijpharm.2004.11.014> PMID: 15652195
48. Maa YF, Nguyen PA, Hsu SW. Spray-drying of air-liquid interface sensitive recombinant human growth hormone. *J Pharm Sci*. 1998; 87(2):152–9. <https://doi.org/10.1021/js970308x> PMID: 9519146.
49. Hancock BC, Zografi G. Characteristics and significance of the amorphous state in pharmaceutical systems. *J Pharm Sci*. 1997; 86(1):1–12. <https://doi.org/10.1021/js9601896> PMID: 9002452.
50. Tang X, Pikal MJ. Design of freeze-drying processes for pharmaceuticals: practical advice. *Pharm Res*. 2004; 21(2):191–200. PMID: 15032301.
51. Levi G, Karel M. Volumetric shrinkage (collapse) in freeze-dried carbohydrates above their glass transition temperature. *Food Research International*. 1995; 28(2):145–51. [http://dx.doi.org/10.1016/0963-9969\(95\)90798-F](http://dx.doi.org/10.1016/0963-9969(95)90798-F).

52. Ho MM, Bolgiano B, Corbel MJ. Assessment of the stability and immunogenicity of meningococcal oligosaccharide C-CRM197 conjugate vaccines. *Vaccine*. 2000; 19(7–8):716–25. PMID: [11115692](#).
53. Perrett KP, Snape MD, Ford KJ, John TM, Yu LM, Langley JM, et al. Immunogenicity and immune memory of a nonadjuvanted quadrivalent meningococcal glycoconjugate vaccine in infants. *Pediatr Infect Dis J*. 2009; 28(3):186–93. <https://doi.org/10.1097/INF.0b013e31818e037d> PMID: [19209097](#).
54. Snape MD, Perrett KP, Ford KJ, John TM, Pace D, Yu LM, et al. Immunogenicity of a tetravalent meningococcal glycoconjugate vaccine in infants: a randomized controlled trial. *JAMA*. 2008; 299(2):173–84. <https://doi.org/10.1001/jama.2007.29-c> PMID: [18182599](#).
55. Borrow R, Richmond P, Kaczmarek EB, Iverson A, Martin SL, Findlow J, et al. Meningococcal serogroup C-specific IgG antibody responses and serum bactericidal titres in children following vaccination with a meningococcal A/C polysaccharide vaccine. *FEMS Immunol Med Microbiol*. 2000; 28(1):79–85. PMID: [10767611](#).
56. Lieberman JM, Chiu SS, Wong VK, Partidge S, Chang SJ, Chiu CY, et al. Safety and immunogenicity of a serogroups A/C *Neisseria meningitidis* oligosaccharide-protein conjugate vaccine in young children. A randomized controlled trial. *JAMA*. 1996; 275(19):1499–503. PMID: [8622225](#).
57. Granoff DM, Maslanka SE, Carlone GM, Plikaytis BD, Santos GF, Mokatrik A, et al. A modified enzyme-linked immunosorbent assay for measurement of antibody responses to meningococcal C polysaccharide that correlate with bactericidal responses. *Clin Diagn Lab Immunol*. 1998; 5(4):479–85. PMID: [9665952](#); PubMed Central PMCID: PMC95603.
58. McIntosh E, Bröker M, Wassil J, Welsch J, Borrow R. Serum bactericidal antibody assays—The role of complement in infection and immunity. *Vaccine*. 2015; 33(36):4414–21. <https://doi.org/10.1016/j.vaccine.2015.07.019> PMID: [26187262](#)
59. Rubinstein LJ, Garcia-Ojeda PA, Michon F, Jennings HJ, Stein KE. Murine immune responses to *Neisseria meningitidis* group C capsular polysaccharide and a thymus-dependent toxoid conjugate vaccine. *Infect Immun*. 1998; 66(11):5450–6. PMID: [9784556](#); PubMed Central PMCID: PMC108682.
60. Chiu SS, Chan KH, Tu W, Lau YL, Peiris JS. Immunogenicity and safety of intradermal versus intramuscular route of influenza immunization in infants less than 6 months of age: a randomized controlled trial. *Vaccine*. 2009; 27(35):4834–9. <https://doi.org/10.1016/j.vaccine.2009.05.066> PMID: [19523908](#).
61. Wahl M, Hermodsson S. Intradermal, subcutaneous or intramuscular administration of hepatitis B vaccine: side effects and antibody response. *Scand J Infect Dis*. 1987; 19(6):617–21. PMID: [3441747](#).
62. Zhang L, Wang W, Wang S. Effect of vaccine administration modality on immunogenicity and efficacy. *Expert Rev Vaccines*. 2015:1–15. <https://doi.org/10.1586/14760584.2015.1081067> PMID: [26313239](#).